4-2016

# Identification and Characterization of Ion Channel Activity of the M2 Protein from Influenza Virus D (DM2)

Jianing Liu
*University of Nebraska-Lincoln*, jianing@huskers.unl.edu

# IDENTIFICATION AND CHARACTERIZATION OF ION CHANNEL ACTIVITY OF THE M2 PROTEIN FROM INFLUENZA VIRUS D (DM2)

by

Jianing Liu

A THESIS

Presented to the Faculty of

The Graduate College at the University of Nebraska

In Partial Fulfillment of Requirements

For the Degree of Master of Science

Major: Biological Sciences

Under the Supervision of Professor Hideaki Moriyama

Lincoln, Nebraska

April, 2016

# IDENTIFICATION AND CHARACTERIZATION OF ION CHANNEL ACTIVITY OF THE M2 PROTEIN FROM INFLUENZA VIRUS D (DM2)

Jianing Liu, M.S.

University of Nebraska, 2016

Advisor: Hideaki Moriyama

Viral ion channels are membrane proteins of influenza viruses that play essential roles in the replication cycle, which enables them to be targeted by antiviral drugs. M2 of influenza type A virus, BM2 of influenza type B virus, and CM2 from influenza type C virus have been characterized as ion channel proteins and antiviral drug amantadine was developed to control influenza type A virus. However, few studies have been conducted to clarify the properties of the M2 protein (DM2) of influenza type D virus, a novel influenza virus genus identified in 2014. To identify the ion channel activity of DM2, we expressed DM2 in the oocytes of *Xenopus laevis* and measured the whole cell currents using the two-microelectrode voltage clamp method. While CM2 exhibited ion channel activity in the *Xenopus* oocyte as a control, DM2 also expressed the ion channel capability in the independent test. In addition, according to the clamping data of the oocytes expressing DM2, the current–voltage relationship was nonlinear, but it was a sigmoid curve as the function of hyperpolarization. These results suggest that DM2 forms a voltage-gated ion channel as CM2 does.

## Table of Contents

## FIGURES AND TABLES

# Chapter I LITERATURE REVIEW

## Influenza viruses

Influenza viruses are negative-sense, single-stranded RNA viruses belonging to the *Orthomyxoviridae* family. There are five genera in *Orthomyxoviridae* family: Influenza virus A, Influenza virus B, Influenza virus C, Thogovirus, and Isavirus (Alexander, 2007). Influenza viruses and Thogovirus have been established for a long time, and Isavirus was relatively newly found. The C/OK viruses, provisionally identified as a subtype of Influenza C virus (ICV), have been characterized as distinct from ICV (Hause, 2014). Therefore, a sixth genus named Influenza D virus will soon be created (Hause, 2014). Influenza A, B, and C cause influenza in a variety of vertebrate species, including human, avian species, and other animals. Influenza D has only been isolated in swine and cattle so far; however, it also has potential threaten to human health as these animals are a potential virus reservoir. The classification of influenza viruses into separate genera is based on two major internal proteins of influenza virus: nucleoprotein (NP) and matrix (M) protein. Influenza A is further classified into subtypes on the basis of the nature of their surface glycoproteins, namely, hemagglutinin (HA) and neuraminidase (NA) (Lamb R. K., 2001). To date, 18 different Hemagglutinin (H1– H18) antigens and 11 different neuraminidase (N1– N11) have been isolated. Each virus subtype has one hemagglutinin and one neuraminidase, and in theory, 198 different combinations are possible.

Two different strategies, vaccination and chemotherapy, have been used to combat influenza. H1N1 and H3N2 of influenza A as well as influenza B were selected to produce vaccination for human use (Manzoli, 2012). However, the effectiveness of vaccination is limited due to antigenic drifts and shifts. The M2 protein of influenza A,

which is an ion channel membrane protein permeable to protons, is the major target of antiviral drugs. Therefore, the anti-influenza drugs are only effective against influenza virus A strains.

**Ion channel proteins**

Ion channels are membrane proteins that gate the flow of ions across the cell membrane by forming water-filled pores (Fischer W. S., 2002). Ion channels can provide a high conducting, hydrophilic pathway across the low dielectric, hydrophobic interior of the phospholipid bilayers (Hille, 2001). They are distinguishable from aqueous pores on account of their ion selectivity and gating activity. Ion channels can discriminate between size and charge of permeant molecules and control their passage rate through the selectivity filter. In addition, ion channels are gated, allowing them to temporarily open in response to a specific stimulus and close again (Figure 1). The main types of stimuli include voltage gradient across the membrane, binding of a ligand (extracellular or intracellular ligand), and mechanical stress (Hille, 2001). The stimulation causes a conformational change in channel protein structure, which results in the opening of the channel gate, ultimately leading to the succeeding ion flux across the plasma membrane. Viral ion channel proteins are short auxiliary membrane proteins with a length of 50–120 amino acids. They have been found in a number of viral genomes and play essential roles in the virus replication cycle, such as virus entry, assembly, and release, by changing the electrochemical or proton gradient in the subcellular compartments in host cells (Wang K. X., 2011). One of the main reasons for the focus on ion channel proteins in influenza viruses is that they can be ideal targets for antiviral drugs, due to their importance in the virus life cycle (Clercq, 2006; Ohigashia, 2009). The basic principle for the inhibition of

ion channel proteins is to either inhibit the channel activity or the assembly of the channel itself (Wang K. X., 2011). The ion channel proteins identified in influenza A, B, and C are designated as M2, BM2, and CM2, respectively, the functions and structures of which will be discussed in the following sections.

**M2 protein of influenza A**

M2 is a single-pass, $N_{in}C_{out}$ oriented membrane protein that consists of 97 amino acids (Pinto, 1992). It is produced from the spliced mRNA transcript that shares a high similarity with that of Matrix 1 protein. M2 is composed of an N-terminal ectodomain (residues 1–23), a transmembrane domain (residues 24–46), and a C-terminal cytoplasmic domain (residues 47–79). The native state of M2 is a homo-tetramer that consists of a pair of dimers covalently linked by disulfite bonds. M2 forms a pH-gated proton channel in the viral lipid envelope. The activation of M2 depends on the low pH of an endosome, and the following conductance is controlled by the inter-subunit interaction between histidine 37 and tryptophan 41. The high proton conductivity is conferred by histidine 37, and the channel gate is conferred by tryptophan 41 (L.H. Pinto, 1997). At high pH, the tryptophan gate is locked through the interaction with Aspartic acid 44, and the transmembrane helices are tightly packed. At low pH, the imidazole ring of His 37 is protonated (Okada, 2001), which destabilizes the transmembrane helix packing and breaks the interactions between Trp 41 and Asp 44, allowing the gate to flip open (Thomaston J.L., 2015).

M2 plays an essential role in viral infection and successful replication in host cells by modulating the pH across the membrane during the entry of virus particles and across the trans-Golgi membrane during viral maturation (McCown, 2006). Influenza A viruses

enter the host cell by expressing M2 protein in the plasma membrane (Schnell, 2008). As a consequence, the host cell incorporates this section of membrane through the endocytosis pathway with virions entrapped in the endosome and employs ATPases to acidify this compartment. Sensing the low pH in the endosome, M2 mediates the change of pH by conducting protons into the interior of the virion, which enables conformational changes of the virus membrane proteins such as hemagglutinin and Matrix 1 protein (Sakaguchi, 1997). As a result, the viral membrane fuses with the endosomal membrane, and the viral genome is released to the host cell. In addition, during the late stage of the infectious cycle for influenza A, M2 is responsible for maintaining a neutral pH in the Golgi, which in turn prevents HA from adopting the low-pH structure that may cause the assembly of nonfunctional HA in the virion (Ciampor, 1992). Based the importance of M2 protein in the influenza virus replication cycle, this protein has been a target for influenza drug development (Fischer W. B., 2012). In the presence of 1-aminoadamantane hydrochloride, an inhibitor of M2 ion channel activity, protons fail to enter the virion, which then cannot disintegrate from the endosome, thus blocking the influenza A viruses from taking over the host cell (Pielak, 2009; Wang C. T., 1993).

**BM2 protein of influenza B**

The influenza B virus BM2 protein contains 109 amino acid residues and is translated from a +2 nucleotides open reading frame. The initiation codon of BM2 overlaps with the stop codon of the M1 protein, indicating that BM2 synthesis is triggered by the termination of M1 translation (Horvath, 1990). BM2 is a type III integral membrane protein with a $N_{out}C_{in}$ orientation and comprises a 23-residue transmembrane domain as well as an 86-residue C-terminal cytoplasmic domain. Like M2 from influenza A, BM2

forms a proton channel, which is activated at acidic pH. In addition, BM2 is a homotetramer in its native state and is involved in the virus uncoating process in the endosome (Paterson, 2003). It is post-transcriptionally modified by phosphorylation, incorporated into virions, and expressed on the membrane of virus-infected cells (Odagiri, 1999). Although M2 and BM2 share no sequence similarity in the transmembrane domain, the HXXXW motif is found in both of them. Histidine 19 and tryptophan 23 of the BM2 protein are essential for pH sensing and channel gating, as are the corresponding proteins, histidine 37 and tryptophan 41, of M2 protein (Otomo, 2009). However, the activity of BM2 is completely insensitive to the anti-influenza drugs amantadine and rimantadine (Mould, 2003 ).

**CM2 protein of influenza C**

CM2 is an integral membrane glycoprotein that forms homodimers and homotetramers linked by disulfite bonds. It is generated by proteolytic cleavage of a 374-amino acid P42 protein, which is composed of a 259-amino acid N-terminal matrix protein (M1) and a 115-amino acid C-terminal CM2 protein (Hongo S. S., 1999). CM2 has a $N_{out}C_{in}$ orientation in membranes with a 23-residue N-terminus extracellular domain, a 23-residue transmembrane domain, and a 69-residue C-terminal cytoplasmic domain (Furukawa, 2011). It is post-translationally modified by palmitoylation through a labile thioester linkage, by N-glycosylation via addition of an N-linked oligosaccharide chain and by phosophorylation (Hongo S. S., 1997; Li, 2001). CM2 forms a voltage-activated ion channel that is permeable to chloride ions and perhaps protons (Hongo S. I., 2004; Muraki Y, 2009). Unlike M2 of influenza A, CM2 is not sensitive to the antiviral drugs amantadine and rimantadine. CM2 is expressed at the plasma membrane of virus-infected

cells and incorporated into virions. It is crucial to the influenza C replication by playing a role in the uncoating and packaging processes. The mechanism how the CM2 channel activities relate to their roles remains unclear and needs further investigation.

**Electrophysiological recording**

*Xenopus* oocytes have been widely used for studying ion channel proteins *in vivo* because of the unique advantages of the oocytes (Weber, 1999), such as their large size, relative ease of handling, and low expression of endogenous channels and receptors. Electrophysiology is considered the most sensitive approach to study ion channel function with the use of *Xenopus* oocytes. Among the electrophysiological techniques, the two-microelectrode voltage clamp (TEVC) method, which studies the properties of electrogenic membrane proteins by artificially controlling the membrane potential, is the most common one for electrophysiological investigation in voltage clamping large cells (Guan, 2013). In combination with various biological approaches, the *Xenopus* oocyte expression system and TEVC are employed to study the structure and function of ion channels and receptors.

Two-electrode whole-cell voltage clamping of oocytes makes use of two intracellular electrodes, with one of them measuring the internal potential of the oocyte as a $V_m$ sensor and the other injecting current to change the membrane potential to a desired value (Figure 2). Both electrodes are interconnected through a feedback amplifier and gently injected into the cell membrane to artificially control membrane potential (Baumgartner, 1999). The membrane potential measured by the $V_m$ sensor is compared with a command voltage, and the difference between them is manipulated by the amplifier to force a current proportional to that difference to flow through the current electrode into the cell

(Polder & Swandulla, 2001). Thus, the difference between the voltages is brought to zero, and the cell membrane potential is clamped at a constant value. With the opening of the ion channel, deviations from the clamped membrane potential are corrected by ions entering through the clamp electrode. By measuring the injected currents at different clamped membrane potential, voltage-gated ion channels can be characterized.

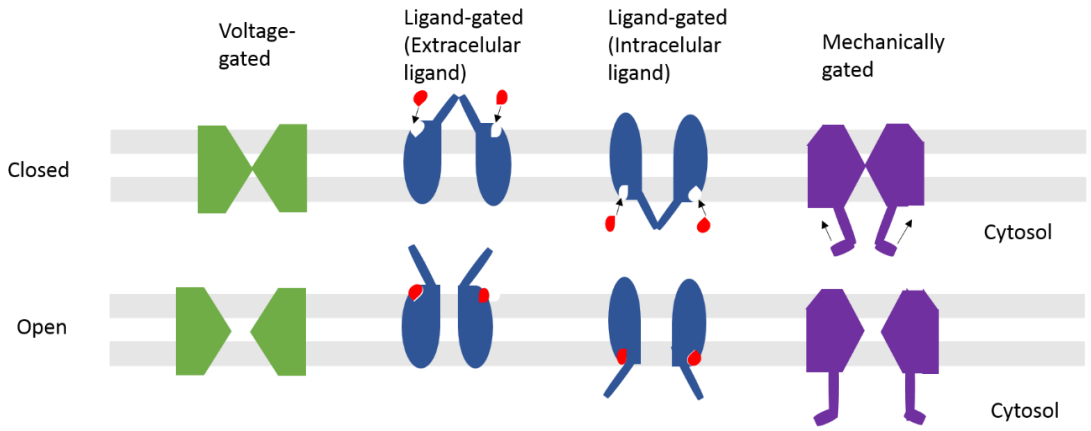


**Figure 1. The gating of ion channels.** Ion channels are gated by a variety of cellular changes, such as the voltage gradient across the membrane, the binding of a ligand (extracellular ligand or intracellular ligand), and a mechanical stress. The ion channels can conduct electrical current by allowing ions to pass through in an open state.

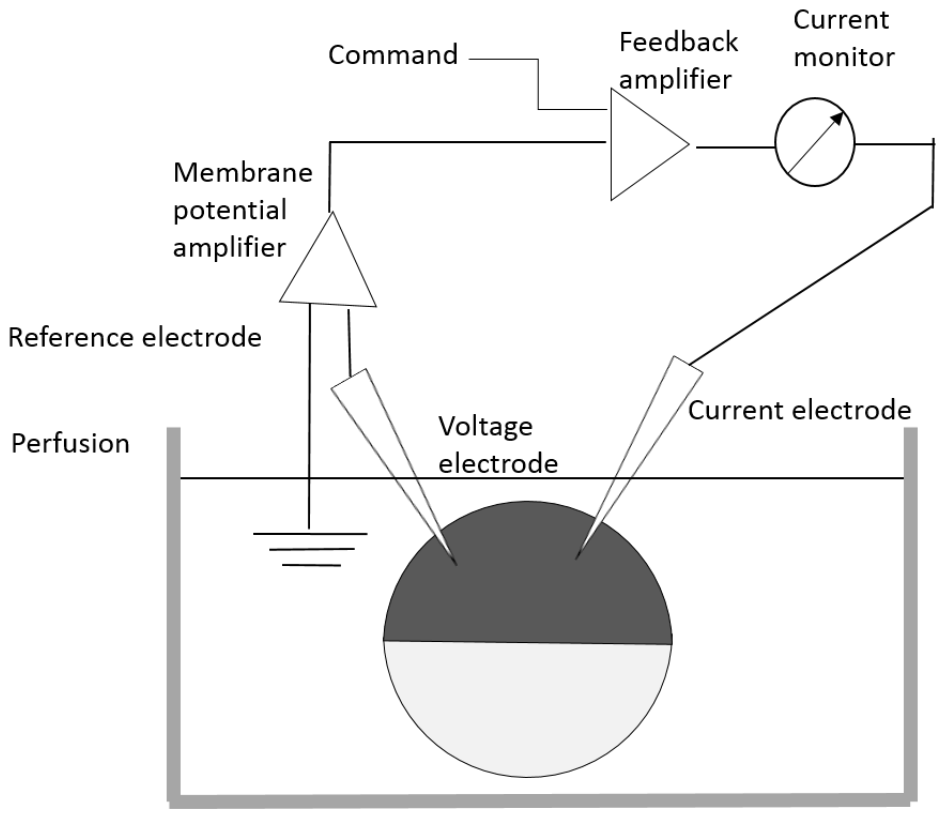


**Figure 2. Diagram of the two- microelectrode voltage clamp (TEVC) on an oocyte.** The oocyte is placed under the dissecting microscope and gently injected with two electrodes filled with conductive solution using micromanipulators. One electrode monitors $V_m$, and the other is used to inject current to adjust $V_m$ to the desired values.

# Chapter II MATERIALS AND METHODS

## Plasmid construction

Plasmid pNCB1 (Figure 3), which contains a T7 promoter for *in vitro* cRNA transcription, as well as the 5′ and 3′ untranslated regions of Xenopus β-globin gene for protein expression in *Xenopus laevis*, was designed by Dr. H. Moriyama and synthesized by GeneScript. The CM2 and DM2 gene products were synthesized and subcloned to vector pNCB1, at the BamHI/XbaI and SmaI/XbaI location of the multiple cloning site of pNCB1, respectively.

## *In vitro* synthesis of mRNA

The mRNA transcripts that contain open reading frames coding for CM2 and DM2 were synthesized *in vitro* with mMESSAGE mMACHINE Kit (Ambion). The recombinant plasmids pNCB1–CM2 and pNCB1–DM2 were linearized downstream of the 3′UTR of Xenopus β-globin gene with restriction enzyme PciI (NEB) and purified with phenol/chloroform extraction and ethanol precipitation. The linearized plasmids were used as templates for the synthesis of capped RNA (cRNA). The *in vitro* transcription reaction was performed according to the instructions of mMESSAGE mMACHINE Kit (Ambion) and incubated at 37°C for 2 h. Template DNA was removed with TURBO DNase (supplied with kit), and the synthesized cRNA was recovered by phenol: chloroform extraction and isopropanol precipitation. The purified cRNA was then suspended in 20 µl nuclease-free $H_2O$, followed with quantitation by gel electrophoresis. Typically about 0.5 µg/µl RNA solution was obtained after purification.

**Injection of oocytes with mRNA**

Defolliculated oocytes (Stage V and VI) were purchased from *Xenopus* 1 and stored in MBSH solution (88 mM NaCl, 1 mM KCl, 2.4 mM $NaHCO_3$, 15 mM HEPES, 0.3 mM $CaNO_3$, 0.33 mM $CaCl_2$, 0.81 mM $MgSO_4$, 10 µg/mL penicillin, and 10 µg/mL streptomycin, pH 7.4). The oocytes with good contrast between the animal hemisphere and vegetal hemisphere were selected using a dissecting microscope and stored on ice prior to injection. The injection needle was obtained by pulling micropipettes (Drummond L = 3.5 inches, OD = 1.14 mm, ID = 0.53 mm) with the Flamming/Brown Micropipette Puller (Model P-97 Sutter Instrument). A 3–5 µm opening at the tip of the injection needle was made with tweezers and sterile mineral oil was filled into the needle with a 1 ml syringe. The needle was then filled with 2 µl cRNA sample solution through a microinjector set on aspiration mode (Figure 4). The oocytes were microinjected in the vegetal hemisphere with 50.6 nl cRNA at a speed of 23 µl/s. The injected oocytes were transferred to a multi-well petri dish plate filled with MBSH solution and incubated at 16°C degree for 3–5 days. The oocyte incubation solution was changed every day after injection.

**Electrophysiological recordings**

Two-electrode voltage clamp experiments were carried out to measure whole-cell oocyte currents. Oocytes were placed in a recording chamber and were perfused with continuous MBSH solution. The recording pipettes were obtained by pulling micropipettes (Sutter L = 3.5 inches, OD = 1.0 mm, ID = 0.50 mm) with the Flamming/Brown Micropipette Puller (Model P-97 Sutter Instrument) and filled with sterile 3 M KCl solution. For the current electrode and voltage electrode pipettes, the tip was broken with fine forceps until

a tip resistance of 1 MΩ was achieved. With the voltage potential set to −60.0 mV, the oocytes were impaled separately with voltage and current electrodes. The impaled oocytes were voltage clamped using the OC-725C-V oocyte clamp amplifier (Warner Instruments) at a slow clamp mode (Figure 5). The clamped membrane potential was observed as the voltage amplitude was adjusted from −80 mV to −160 mV in 10 s pulses. The membrane potential was held at −60 mV, and the currents were low pass-filtered at 1 kHz. PL3508B75-V PowerLab system (ADInstruments) was used for the data recording and signal processing. All electrophysiological recordings were carried out at room temperature.

**Isolation of plasma membrane complexes from *Xenopus* oocytes**

*Xenopus* oocytes, 2–3 days post-injection, were used for the isolation of plasma membrane fraction. Five oocytes were rinsed in MES-buffered saline solution (MBSS; 20 mM MES, 80 mM NaCl, pH 6.0) and incubated at room temperature for 10 min. The following polymerization steps were performed at 4°C under mild agitation. The oocytes were first rotated in MBSS solution with 1% colloidal silica for 30 min and rinsed thoroughly in MBSS solution, followed by the rotation of oocytes in MBSS solution with 0.1% polyacrylic acid for 30 min and thoroughly washed in MBSS solution. The oocytes were then homogenized in an Eppendorf tube with 1200 µl HbA (20 mM Tris, 5 MM $MgCl_2$, 5 MM $NaH_2PO_4$, 1 MM EDTA, 80 mM sucrose, 1 mM PMSF, 5 µg/ml leupeptin, 5 µg/ml peptatin, pH 7.4) and centrifuged for 30 s at 13.5 g. The top 1 ml supernatant was removed after centrifugation and replaced with the same amount of fresh HbA. This process was repeated four times and the supernatant were centrifuged at 13.5, 13.5, 24, and 38 × *g*, respectively. A final centrifugation at max speed for 20 min was performed to

pellet the purified plasma membranes, which were then resuspended with 10 µl HbA buffer.

**Mass spectrometry of purified plasma membrane complexes**

Protein samples with purified plasma membrane complexes were sent to the Nebraska Center for Mass Spectrometry (Lincoln, NE) for protein identification using tandem mass spectrometry with a Waters Q-TOF Ultima mass spectrometer (Micromass/Waters, Milford, MA). Extracted protein samples were sonicated 1 min at 0°C, reduced with 2 mM DTT at 37°C for 1 h, diluted with 50 MM ammonium bicarbonate, and digested with 10 ng/µl trypsin *in situ*. The samples were then concentrated with two 60 µl aliquots of 1:1 acetonitrile:water (v/v) containing 1% formic acid and subjected to a C18 reversed phase column (75 µm × 15 cm; LC-Pacings, Dionex, Sunnyvale, CA). The acquired MS/MS data were searched against the NCBI protein database with the significance threshold set at $P < 0.05$.

**Sequence alignment and transmembrane domain prediction**

Protein sequences of M2 (GI 89033149), BM2 (GI 51340786), CM2 (GI 27531632), and DM2 (685509396) were identified by searching against the NCBI (National Center for Biotechnology Information) database and aligned using MAFFET 7.0 with default settings (BLOSUM62 scoring matrix, gap opening penalty 1.53, offset value 0.0, leave gappy regions). TMHMM Serer v.2.0 was used to predict the transmembrane helices in proteins with default settings (Output format, Extensive, with graphics).

**Molecular modeling**

Swiss-Model was used to generate the molecular structure modeling of the transmembrane domain of target protein DM2. The NMR structure of BM2 (PDB: 2KIX)

was employed as the template and the sequence alignment between DM2 and BM2, performed by ClustalW alignment, was also used as input for the modeling process.

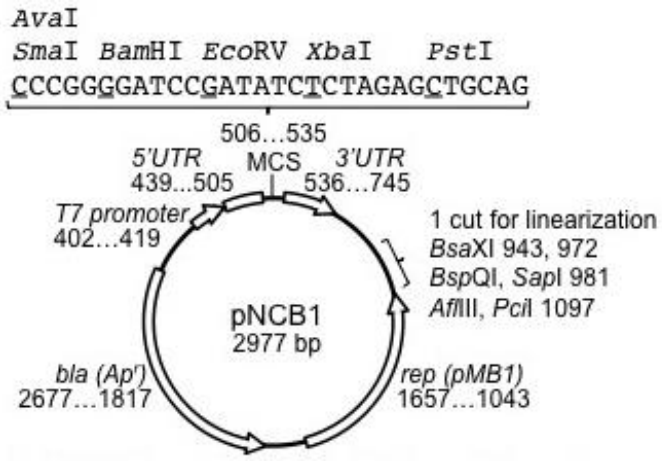


**Figure 3. Plasmid pNCB1 construction. pNCB1 was derived from vector pGEM–HE and vector pUC57.** It contains the 5′ and 3′ UTR from Xenopus β-globin gene, which are involved in the regulation of protein translation in oocytes, and T7 promoter that can be recognized by T7 polymerase during cRNA transcription. DNA of interest can be subcloned into MCS, which includes the SmaI, BamHI, EcoRV, XbaI, and PstI restriction cutting sites. Restriction enzymes PciI, BsaXI, BpQI, SapI, and AffIII can be used for plasmid linearization.

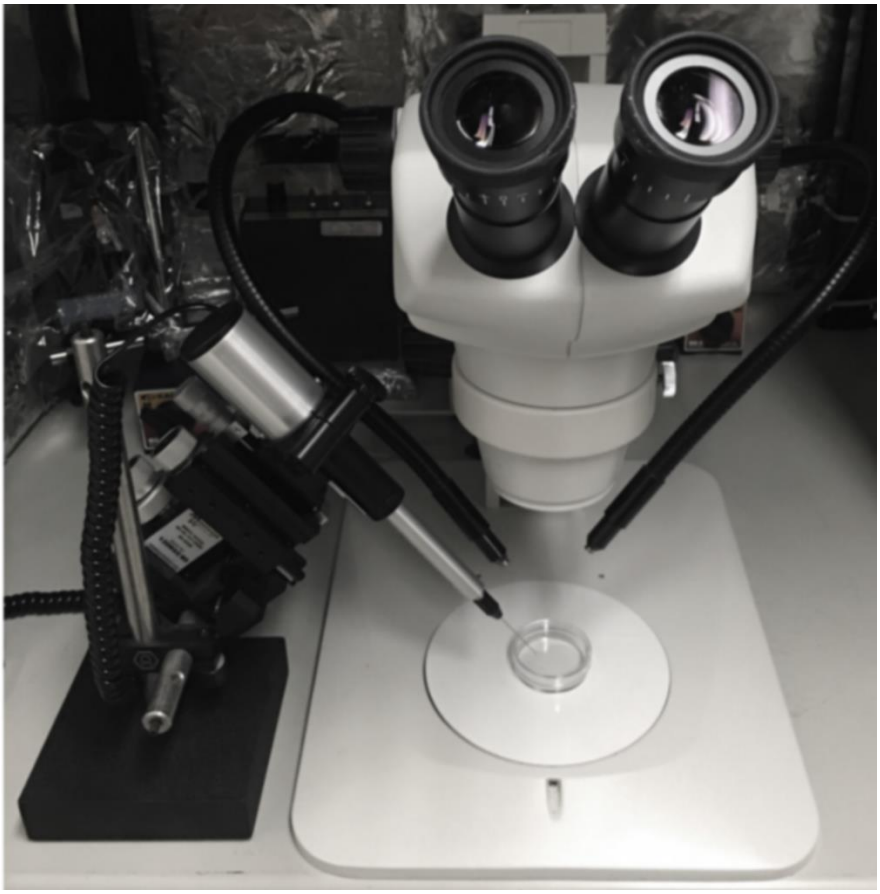

**Figure 4. Apparatus for cytoplasmic injection of Xenopus oocytes.** The oocytes were placed on a 35-mm tissue culture dish on the stage of a dissecting microscope. The injection needle, pulled with micropipette puller, was filled with approximately 2 µl RNA solution and was positioned over individual oocytes using a micromanipulator.


**Figure 5. Apparatus for the measurement of the whole-cell currents of *Xenopus* oocytes using the two-electrode voltage clamp method.** The voltage electrode and current electrode were placed on a micromanipulator and positioned over an oocyte, which was placed in a perfusion chamber. Both electrodes were connected to a feedback amplifier.

# Chapter III DETECTION AND CHARACTERIZATION OF THE ION CHANNEL ACTIVITY OF DM2 IN *XENOPUS LAEVIS* OOCYTES

## Study design

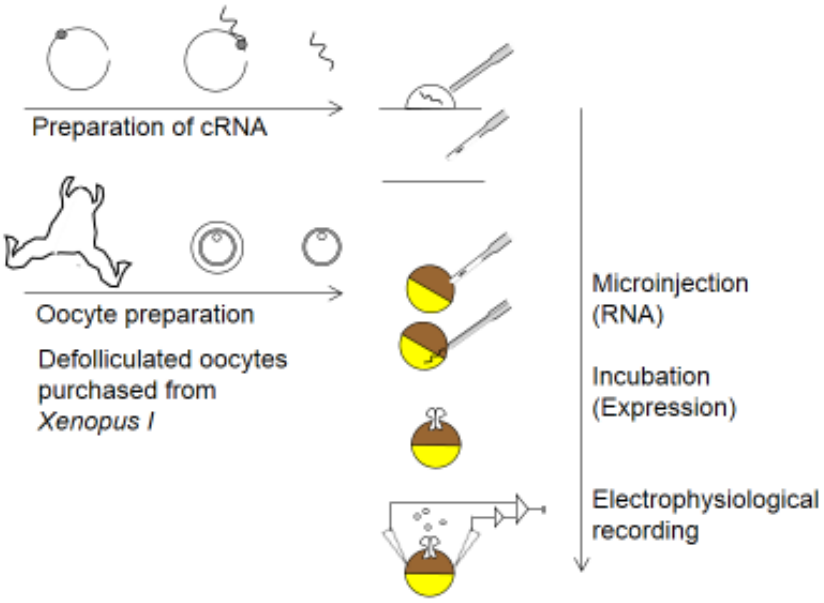


To characterize the ion channel activity of DM2 protein, we employed the *Xenopus laevis* oocyte expression system combined with the electrophysiological recording system to conduct the study. Capped mRNAs of the DM2-ORF (open reading frame) were injected to the defolliculated *Xenopus* oocytes of stage V and VI, which were further incubated in MBSH solution for around 3 days. After the DM2 protein was expressed in the oocytes, two-electrode voltage clamp method was used to do the electrophysiological recording.

## In vitro cRNA synthesis

The pNCB1–CM2 and pNCB1–DM2 plasmids were linearized with restriction enzyme PciI (Figure 6) and used as the template for the *in vitro* capped mRNA synthesis of CM2 and DM2. The synthesized cRNA samples of CM2 and DM2 were purified and examined

by gel electrophoresis (Figure 7). Both CM2-ORF and DM2-ORF transcripts were single-stranded RNAs and around 550 base pairs.

**Expression of CM2 and DM2 in oocytes**

To confirm that CM2 and DM2 protein are synthesized in oocytes of *Xenopus laevis* that were injected with CM2-ORF and DM2-ORF transcripts, the plasma membrane proteins of oocytes were extracted and examined by mass spectrometry.

**Detection and characterization of the ion channel activity DM2**

To determine whether DM2 has ion channel activity, *Xenopus* oocytes injected with CM2 mRNA, DM2 mRNA, and plasmid pNCB1 DNA were incubated in MBSH solution for 3–5 days and used for the measurement of whole cell currents by two-electrode voltage clamp method. The membrane potential was held at −60 mV, and test pulses were imposed from −80 to −160 mV in 10 mV increments (Figure 8). The currents that flowed at the end of the hyperpolarizing pulse from −80 mV to −160 mV were recorded (Table 1). The whole cell currents of three oocytes for each sample were selected and plotted against membrane voltages (Figure 9). For the uninjected oocytes and pNCB1 plasmid DNA injected oocytes, the membrane currents induced upon hyperpolarization pulse were extremely low, varying from −0.5 to −0.8 μA. As to the CM2 mRNA and DM2 mRNA injected oocytes, the membrane currents upon hyperpolarization from −80 mV to −100 mV were relatively low, similar to those of the uninjected and pNCB1 vector DNA injected oocytes. However, for the membrane currents upon hyperpolarization from −110 mV to −160 mV, we can clearly see that the values increased almost 4–5 times compared with the currents induced from −80 mV to −100 mV. The curve of the current–voltage

relationship for oocytes expressing DM2 almost overlaps with that of CM2, indicating that DM2 has similar ion channel activity with CM2 protein.

**Sequence alignment and motif prediction**

The protein sequences of M2, BM2, CM2, and DM2 were aligned using MAFFET 7.0, and the transmembrane (TM) domain prediction was accomplished with TMHMM Serer v.2.0. According to the alignment and TM prediction results, HXXXW motif existed in the transmembrane domains of M2 and BM2, consistent with previous studies. In addition, corresponding to the HXXXW motif in M2 and BM2, an YXXXK motif was identified in transmembrane domains of CM2 and DM2 (Figure 10). For CM2 protein, tyrosine is located at position 67 and lysine is located position 71. As to DM2, tyrosine amino acid was found in position 72 and lysine in position 76. The tyrosine amino acid in YXXXK motif may play the role of tryptophan, which is responsible for the channel gate, and the lysine amino acid could be the counterpart of histidine, conferring the ion conductivity.

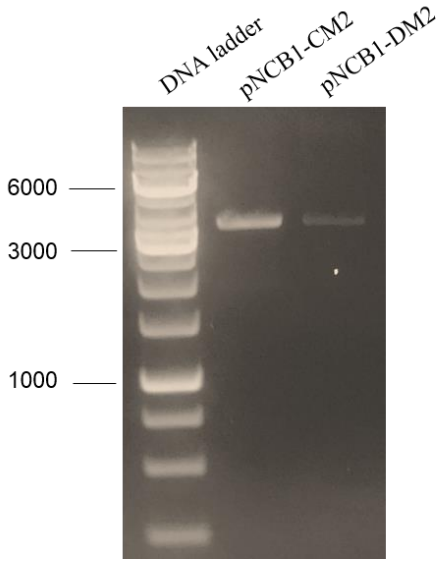


**Figure 6. Linearization of plasmids by PciI restriction enzyme.** pNCB1–CM2 and pNCB1–DM2 were digested with restriction enzyme PciI and purified phenol/chloroform extraction and ethanol precipitation, followed by the gel electrophoresis analysis. DNA ladder is indicated at the left of the gel (in bp).

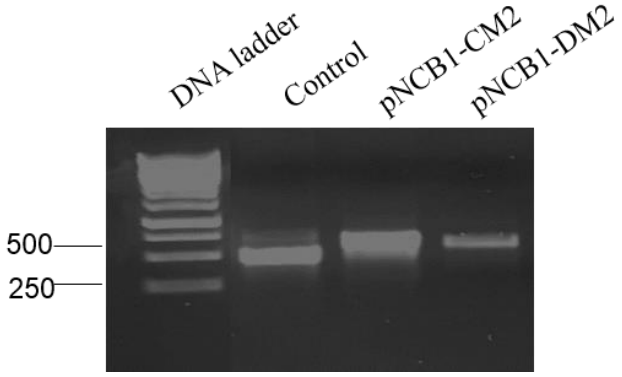


**Figure 7. In vitro capped mRNA synthesis.** The linearized plasmids pNCB1–CM2, pNCB1–DM2 and control (pTRI–Xef1) were used as templates for the synthesis of capped mRNA. The in vitro transcription reaction was performed with mMESSAGE mMACHINE Kit (Ambion) kit. The synthesized CM2 and DM2 cRNA samples were recovered and suspended with 20 µl nuclease-free $H_2O$, followed with quantitation by gel electrophoresis. DNA ladder (in bp) is indicated at the left of the gel.

**Table 1. The membrane currents of oocytes induced upon hyperpolarization.**

| | Whole Cell Currents ((μA) evoked by voltage clamping | | | |
|---|---|---|---|---|
| Clamping voltage (mV) | Uninjected | pNCB1 DNA injected | CM2 mRNA injected | DM2 mRNA injected |
| -80 | -0.51 | -0.51 | -0.51 | -0.51 |
| -90 | -0.53 | -0.54 | -0.78 | -0.56 |
| -100 | -0.53 | -0.64 | -1.02 | -0.65 |
| -110 | -0.61 | -0.67 | -1.34 | -0.97 |
| -120 | -0.62 | -0.72 | -1.64 | -1.14 |
| -130 | -0.69 | -0.81 | -1.96 | -1.36 |
| -140 | -0.71 | -0.82 | -2.07 | -1.52 |
| -150 | -0.79 | -0.96 | -2.19 | -1.85 |
| -160 | -0.83 | -1.05 | -2.51 | -2.13 |

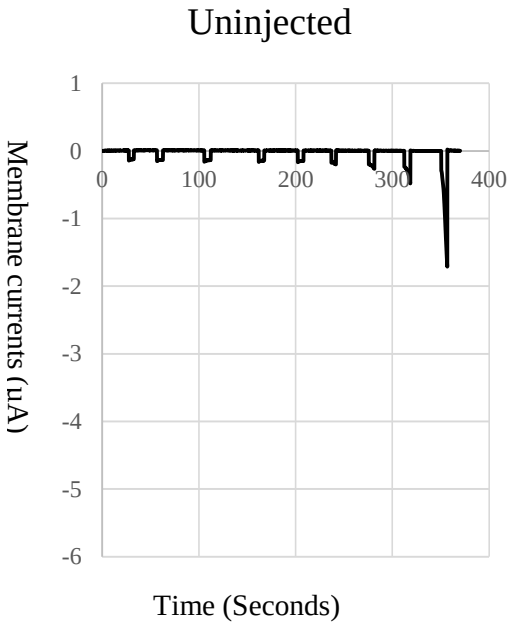
Uninjected
Membrane currents (uA)
1
0
-1
-2
-3
-4
-5
-6
0
100
200
300
400
Time (Seconds)

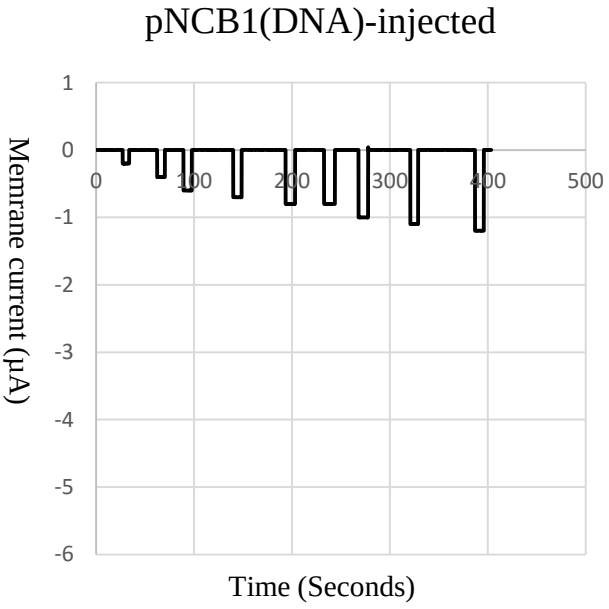
pNCB1(DNA)-injected
Memrane current (μA)
1
0
-1
-2
-3
-4
-5
-6
0
100
200
300
400
500
Time (Seconds)

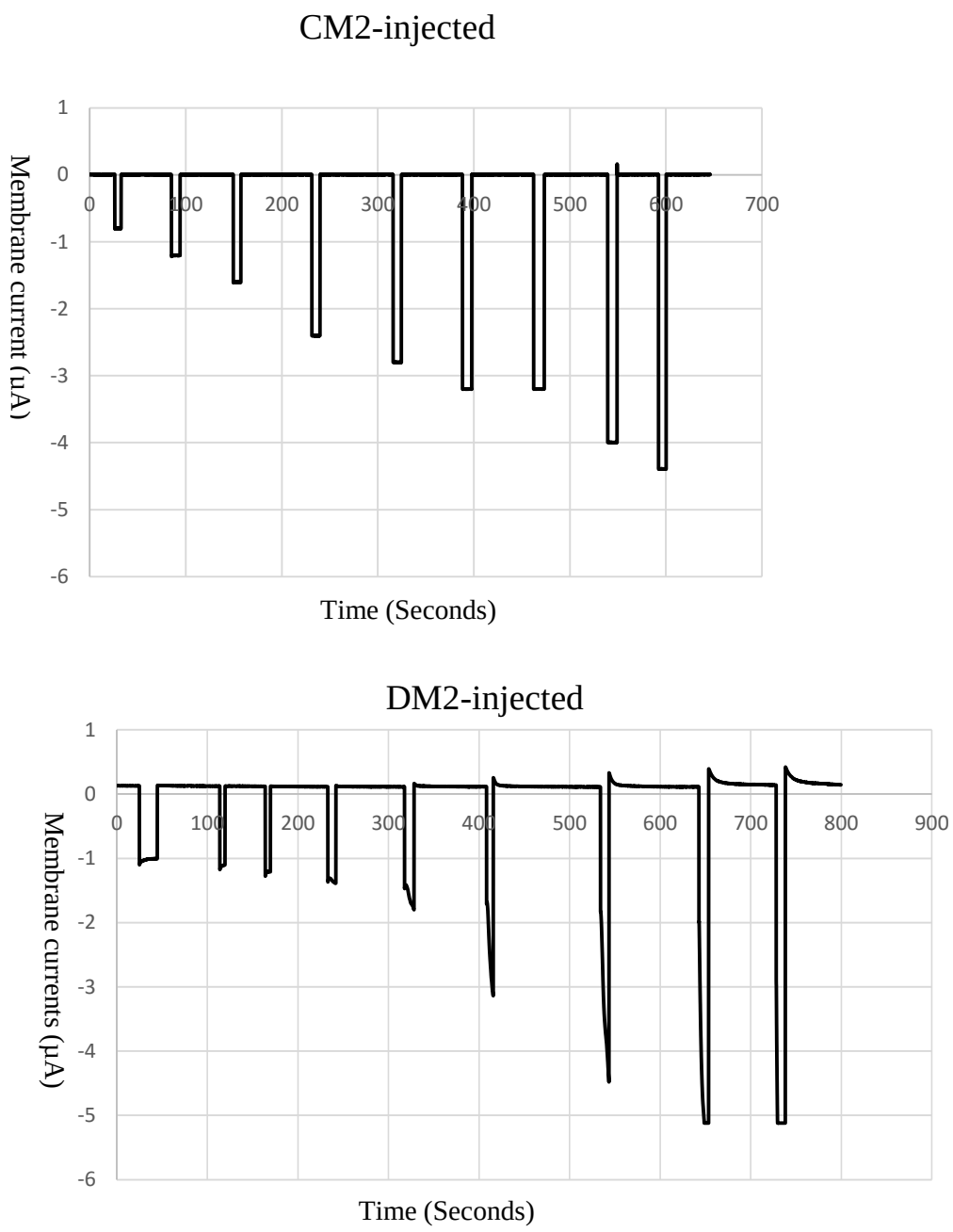


**Figure 8. Original recording file of membrane currents evoked by voltage application over time.** The holding potential was −60 mV, and test pulses were from −80 to −160 mV in 10 mV increments during experiment.

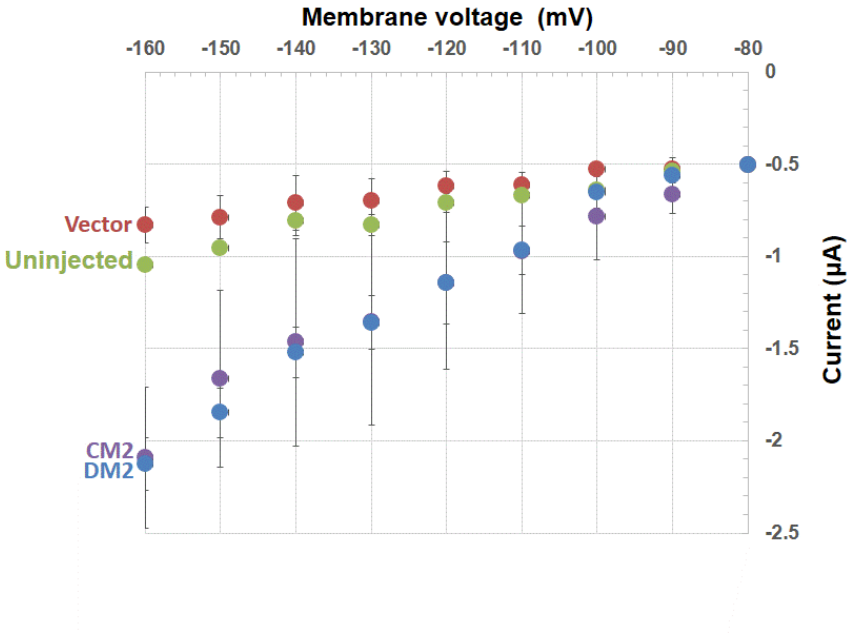


**Figure 9. The current–voltage relationship for oocytes in which the whole-cell current were measured by the two-electrode voltage clamp method.** The oocytes injected with plasmid pNCB1 DNA, CM2 mRNA, DM2 mRNA as well as the uninjected oocytes were incubated in MBSH solution for about 4 days before the measurement. The holding potential was −60 mV, and test pulses were from −80 to −160 mV in 10 mV increments during experiment.

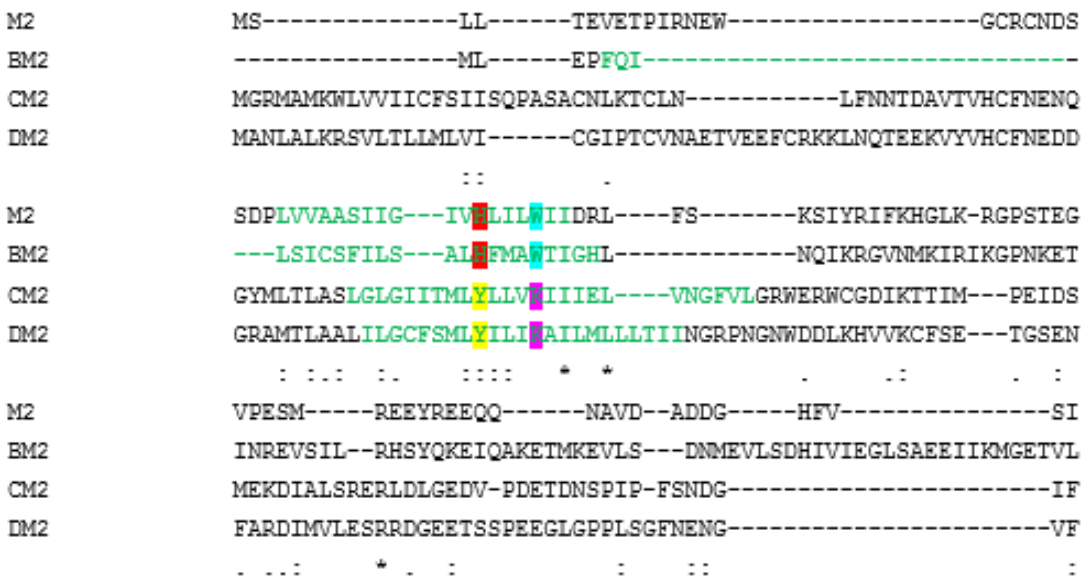


**Figure 10. Sequence alignment of M2, BM2, CM2, and DM2 from influenza virus A, B, C, and D.** Amino acids colored as green are the transmembrane (TM) domains of M2 proteins. HXXXW motif found in M2 and BM2 is essential for channel function, with histidine (red) conferring proton selectivity and tryptophan (blue) responsible for the channel gate. YXXXK motif (yellow and purple) is found in CM2 and DM2, corresponding to the HXXXW motif in M2 and BM2.

## Chapter IV DISCUSSION

Recently, the influenza virus D, a novel influenza virus found in swine and cattle, has been characterized as a new genus in the *Orthomyxoviridae* family (Hause, 2014). Though influenza virus D has been only isolated from swine and cattle, further studies indicate that this pathogen has the potential to cause disease in humans and to threaten human health (Collin, 2014). According to studies of influenza A, B, and C, M2, BM2, and CM2, the ion channel proteins that play an important role in virus replication cycle, are the ideal targets for the antiviral drugs (Clercq, 2006; Ohigashia, 2009). Therefore, the counterpart of the ion channel proteins, DM2 of influenza D, is the potential ion channel protein and may has important impact in the virus replication.

We expressed Influenza D DM2 protein in *Xenopus laevis* oocytes by injecting DM2 mRNA and measured the whole cell current via two-electrode voltage clamp method. The data acquired showed that like M2 protein of influenza A, BM2 protein of influenza B and CM2 protein of influenza C, DM2 exhibits ion channel activity. In addition, on the basis of the characteristic that the current–voltage relationships of oocytes expressing CM2 and oocytes expressing DM2 overlapped with each other, DM2 is likely to form a voltage-gated ion channel, similar to CM2. The similarity of the ion channel activity between CM2 and DM2 is consistent with their close phylogenetic relationship (Lindstrom, 1999). Furthermore, the conclusion that CM2 and DM2 share similar ion channel activity accords with our sequence alignment results, which indicated that the YXXXK motif found in the transmembrane domains of CM2 and DM2 is responsible for channel gating and ion selectivity. It is also supported by the structural model of DM2 (Figure 11), which showed that DM2 forms a left-handed coiled-coil tetramer where the

residues Tyr 72 and Lys 76 pointing toward the pore. Tyr 72 is likely to control the conformational change of the ion channel between opening state and closed state, whereas Lys 76 confers the conductivity of ions. Moreover, the molecular clock analysis of CM2 gene of influenza C viruses isolated in different years showed that the substitution numbers and the year of isolation are not related. Besides, the substitution rate is low, especially for the transmembrane domain, which is essential for the ion channel activity. This can be explained by the importance of CM2 for the influenza C replication cycle. The CM2 gene maintains low substitution rate to keep the ion channel activity and ultimately keep its ability in uncoating and packaging during influenza C replication.

On the other hand, M2 of influenza A and BM2 of influenza B are pH-gated ion channel proteins that acidify the virion interiors in the acidic environment. The HXXXW motif, of which histidine confers the proton conductivity and tryptophan regulates the channel gate, are present in the transmembrane helices of M2 and BM2. At the same time, M2 and BM2 are genetically homogenous and phylogenetically close. Therefore, the tyrosine and lysine in YXXXK motif found in both CM2 and DM2 may play the corresponding role as HXXXW motif in M2 and BM2, with tyrosine monitoring the gate and lysine conferring the ion selectivity.

Our study provides preliminary evidence that DM2 conducts voltage-gated ion channel activity. However, to further characterize the ion channel properties of DM2, we need to identify the ion selectivity of DM2 by changing the solution in which oocytes expressing DM2 are placed in the process of two-electrode voltage clamp experiment. Additionally, the role of YXXXK motif found in CM2 and DM2 can be validated by creating the

mutations in the transmembrane domains of CM2 and DM2. Moreover, the antiviral drugs to influenza D can be developed by testing the impact of certain drugs, such as amantadine and rimantadine, on the ion channel activity of DM2.

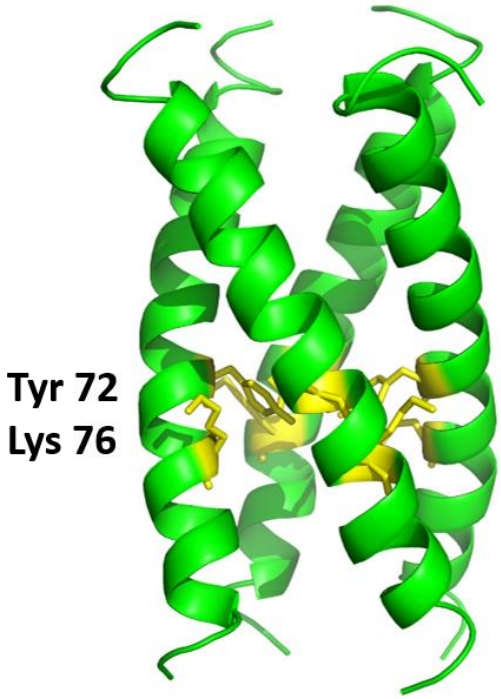


**Figure 11. Diagram of the DM2 transmembrane structure.** The four-transmembrane helix domains are shown as green-colored ribbons. The residues pointing to the center, Tyrosine$^{72}$ and Lysine$^{76}$, are shown in yellow sticks. This figure was created with Swiss-Model.

**References**

Alexander, D. (2007). An overview of the epidemiology of avian influenza. *Vaccine,* 5637–5644.

Baumgartner, W. I. (1999). Two-Microelectrode Voltage Clamp of Xenopus Oocytes: Voltage Errors and Compensation for Local Current Flow. *Biophysical Journal* , 1980–1991.

Ciampor, F. B. (1992). Evidence that the amantadine-induced, M2-mediated conversion of influenza A virus hemagglutinin to the low pH conformation occurs in an acidic trans Golgi compartment. *Virology,* 188, 14–24.

Clercq, E. (2006). Antiviral agents active against influenza A viruses. *Nature Reviews Drug Discovery,* 5, 1015-1025.

Collin, E. S. (2014). Cocirculation of Two Distinct Genetic and Antigenic Lineages of Proposed Influenza D Virus in Cattle. *Journal of Virology,* 1036-1042.

Fischer, W. B. (2012). Mechanism of function of viral channel proteins and implications for drug development. . *Int Rev Cell Mol Biol*, 294, 259–321.

Fischer, W. S. (2002). Viral ion channels: structure and function . *Biochimica et Biophysica Acta* , 27-45.

Furukawa, T. M. (2011). Role of the CM2 Protein in the Influenza C Virus Replication Cycle. *Journal of virology* , 1322-1329.

Guan, B. X. (2013). Two-electrode voltage clamp. *Methods in Molecular Biology,* 998: 79–89.

Hause, B. C. (2014). Characterization of a Novel Influenza Virus in Cattle and Swine: Proposal for a New Genus in the Orthomyxoviridae Family. *mBio*, 00031–14.

Hille, B. (2001). *Ion Channels of Excitable Membranes (3rd ed.).* Sunderland, Mass: Sinauer Associates: Inc. p. 5. ISBN 0-87893-321-2.

Hongo, S. I. (2004). Detection of ion channel activity in Xenopus laevis oocytes expressing Influenza C virus CM2 protein. *Arch Virol*, 149(1):35-50.

Hongo, S. S. (1997). Characterization of a second protein (CM2) encoded by RNA segment 6 of influenza C virus. *Journal of Virology*, 2786–2792.

Hongo, S. S. (1999). Influenza C Virus CM2 Protein Is Produced from a 374-Amino-Acid Protein (P42) by Signal Peptidase Cleavage. *JOURNAL OF VIROLOGY,* 46-50.

Horvath, C. M. (1990). Eukaryotic coupled translation of tandem cistrons: identification of the influenza B virus BM2 polypeptide. . *EMBO J*, 9:2639–2647.

L.H. Pinto, G. D. (1997). A functionally defined model for the M2 proton channel of influenza A virus suggests a mechanism for its ion selectivity. *Proc. Natl. Acad. Sci.*, 11301–11306.

Lamb, R. K. (2001). Orthomyxoviridae: the viruses and their replication. *Fields Virology*, 1487–1532.

Lamb, R. Z. (1985). Influenza virus M2 protein is an integral membrane protein expressed on the infected-cell surface. *Cell*, 40(3):627-33.

Li, Z. H. (2001). The sites for fatty acylation, phosphorylation and intermolecular disulphide bond formation of influenza C virus CM2 protein. *Journal of General Virology*, 1085–1093.

Lindstrom, S. Y. (1999). Comparative Analysis of Evolutionary Mechanisms of the Hemagglutinin and Three Internal Protein Genes of Influenza B Virus: Multiple Cocirculating Lineages and Frequent Reassortment of the NP, M, and NS Genes. *Journal of Virology* , 4413-4426.

Manzoli, L. I. (2012). Effectiveness and harms of seasonal and pandemic influenza vaccines in children, adults and elderly. *Hum Vaccin Immunother*, 851-862.

McCown, M. F. (2006). Distinct domains of the influenza A virus M2 protein cytoplasmic tail mediate binding to the M1 protein and facilitate infectious virus production. *J. Virol.*, 80, 8178–8189.

Mould, J. P. (2003 ). Influenza B virus BM2 protein has ion channel activity that conducts protons across membranes. *Dev Cell*, 175-184.

Muraki Y, H. A. (2009). Establishment of mouse erythroleukemia cell lines expressing complete influenza C virus CM2 protein or chimeric protein consisting of CM2 and influenza A virus M2. *Acta Virol*, 53:125–129.

Odagiri, T. H. (1999). The BM2 protein of influenza B virus is synthesized in the late phase of infection and incorporated into virions as a subviral component. *J. Gen. Virol*, 80, 2573–2581.

Ohigashia, Y. M. (2009). An amantadine-sensitive chimeric BM2 ion channel of influenza B virus has implications for the mechanism of drug inhibition. *Proceedings of the National Academy of Sciences*, 18775–18779.

Okada, A. M. (2001). Protonation of histidine and histidine-tryptophan interaction in the activation of the M2. *Biochemistry*, 40, 6053–60.

Otomo, K. T. (2009). Interactions Between Histidine and Tryptophan Residues in the BM2 Proton Channel from Influenza B Virus. *The Journal of Biochemistry*, 543-554.

Paterson, R. G. (2003). nfluenza B virus BM2 protein is an oligomeric integral membrane protein expressed at the cell surface. nfluenza B virus BM2 protein is an oligomeric integral membrane protein expressed at the cell surface. . *Virology* , 306:7-17.

Pielak, R. M. (2009). Mechanism of drug inhibition and drug resistance of influenza A M2 channel. *Proc Natl Acad Sci*, 106(27): 11425.

Pinto, L. H. (1992). Influenza virus M2 protein has ion channel activity. *Cell*, 69:517–528.

Polder, H., & Swandulla, D. (2001). The use of control theory for the design of voltage clamp systems: a simple and standardized procedure for evaluating system parameters. *Journal of Neuroscience Methods*, 109 (2): 97–109.

Sakaguchi, T. T. (1997). The active oligomeric state of the minimalistic influenza virus M2 ion channel is a tetramer . *Proc. Natl. Acad. Sci.*, 5000–5005.

Schnell, J. C. (2008). Structure and mechanism of the M2 proton channel of influenza A virus. *Nature* , 451, 591-595 .

Thomaston J.L., A.-P. M. (2015). High-resolution structures of the M2 channel from influenza A virus reveal dynamic pathways for proton stabilization and transduction. *Proc Natl Acad Sci* , 112(46):14260-5.

Wang, C. T. (1993). Ion channel activity of influenza A virus M2 protein: characterization of the amantadine block. *J. Virol.*, 5585–5594.

Wang, K. X. (2011). Viral proteins function as ion channels. *Biochimica et Biophysica Acta*, 510-515.

Weber, W. (1999). Ion currents of Xenopus laevis oocytes: state of the art. *Biochim. Biophys. Acta*, 1421, 213–233.